



OPEN

The Roles of Testicular C-kit Positive Cells in *De novo* Morphogenesis of Testis

SUBJECT AREAS:
TISSUE ENGINEERING
SPERMATOGENESIS

Man Zhang^{1,2}, Hai Zhou^{1,3}, Chunxing Zheng⁴, Jun Xiao⁵, Erwei Zuo^{1,6}, Wujuan Liu¹, Da Xie⁷, Yufang Shi⁴, Chunlian Wu³, Hongyan Wang⁵, Dangsheng Li^{8,9} & Jinsong Li^{1,7}

Received
16 April 2014

Accepted
15 July 2014

Published
4 August 2014

Correspondence and
requests for materials
should be addressed to
J.L. (jsli@sibcb.ac.cn)

¹Group of Epigenetic Reprogramming, State Key Laboratory of Cell Biology, Shanghai Key Laboratory of Molecular Andrology, Institute of Biochemistry and Cell Biology, Shanghai Institutes for Biological Sciences, Chinese Academy of Sciences, Shanghai, China, 200031, ²University of Chinese Academy of Sciences, Beijing, China, 100049, ³College of Life Science, China West Normal University, Nanchong, Sichuan, China, 637002, ⁴Key Laboratory of Stem Cell Biology, Institute of Health Sciences, Shanghai Institutes for Biological Sciences, Chinese Academy of Sciences/Shanghai Jiao Tong University School of Medicine, Shanghai, China, 200025, ⁵State Key Laboratory of Cell Biology, Institute of Biochemistry and Cell Biology, Shanghai Institutes for Biological Sciences, Chinese Academy of Sciences, Shanghai, China, 200031, ⁶State Key Laboratory for Conservation and Utilization of Subtropical Agro-Bioresources, Animal Reproduction Institute, Guangxi University, Nanning, Guangxi, China, 530004, ⁷School of Life Science and Technology, Shanghai Tech University, Shanghai, China, 200031, ⁸Institute of Biochemistry and Cell Biology, Shanghai Institutes for Biological Sciences, Chinese Academy of Sciences, Shanghai, China, 200031, ⁹Shanghai Information Center for Life Sciences, Shanghai Institutes for Biological Sciences, Chinese Academy of Sciences, Shanghai, China, 200031.

C-kit positive (c-kit⁺) cells are usual tissue-specific stem cells. However, in postnatal testis, undifferentiated spermatogonial stem cells (SSCs) are c-kit negative (c-kit⁻) and activation of c-kit represents the start of SSC differentiation, leaving an intriguing question whether other c-kit⁺ cells exist and participate in the postnatal development of testis. To this end, a feasible system for testicular reconstitution, in which a specific type of cells can be manipulated, is needed. Here, we first establish *de novo* morphogenesis of testis by subcutaneous injection of testicular cells from neonatal testes into the backs of nude mice. We observe testicular tissue formation and spermatogenesis from all injected sites. Importantly, functional spermatids can be isolated from these testicular tissues. Using this system, we systemically analyze the roles of c-kit⁺ cells in testicular reconstitution and identify a small population of cells (c-kit⁺:CD140a⁺:F4/80⁺), which express typical markers of macrophages, are critical for *de novo* morphogenesis of testis. Interestingly, we demonstrate that these cells are gradually replaced by peripheral blood cells of recipient mice during the morphogenesis of testis. Thus, we develop a system, which may mimic the complete developmental process of postnatal testis, for investigating the testicular development and spermatogenesis.

It is well known that activation of c-kit signaling is critical in cell migration, survival, proliferation, self-renewal and differentiation^{1,2}. Expression of c-kit has been used as a marker for isolating tissue-specific stem cells or progenitor cells, such as hematopoietic stem cells/progenitor cells^{3,4}, cardiac stem cells⁵⁻⁷ and lung stem cells⁸. Interestingly, bone marrow-derived c-kit⁺ cells could promote cardiac repair by stimulation of the activity of endogenous cardiac progenitor cells⁹, indicating that c-kit⁺ cells play key roles in tissue development and regeneration.

Testicular development is a complex process that can be roughly divided into embryonic and postnatal stages. During fetal gonadal development, the expression of c-kit regulates migration, survival and proliferation of primordial germ cells (PGCs)¹⁰⁻¹². The male PGCs become arrested at the G0/G1 of the cell cycle at around 13.5 days post-coitum (dpc) and begin to divide mitotically again around 3 days after birth during which the expression of c-kit is dramatically reduced¹³. Reactivation of c-kit in postnatal testis is detected in differentiating SSCs, but not in undifferentiated SSCs^{14,15}. Furthermore, from c-kit⁻ cell population, SSCs can be highly enriched using several other surface markers¹⁶⁻¹⁸. Taken together, activation of c-kit is not required for SSC self-renewal, but for spermatogenesis. This leaves an open question of whether other c-kit⁺ cells exist and play important roles in postnatal development of testis.

In past decades, a variety of model systems have been developed to recapitulate spermatogenesis and testicular development *in vitro* and *in vivo*¹⁹. However, a feasible system for studying the function of different cells in testicular development is lacking. An emerging technique, in which, testicular cell-derived tissue (TCDT) can be *de novo* formed after ectopic transplantation of cells dissociated from newborn testes into the subcutis of



immunodeficient mice, could mimic the complete process of postnatal testicular development. This technique, termed *de novo* morphogenesis of testis¹⁹, has been used to reconstitute mouse²⁰, rat²⁰, porcine²¹ and sheep²² testes in immunodeficient mice. One intriguingly potential application of this approach is to manipulate different cells prior to grafting¹⁹, providing an opportunity to reveal the function of different cells in postnatal development of testis. However, the efficiency of spermatogenesis in these *de novo*-formed TCDDTs is low^{20,21}, and the functional male gametes could be generated only by integration of exogenous SSCs²⁰, restricting its broad range of applications for studying spermatogenesis and testicular development.

In this study, we modified the process of grafting testicular cells and obtained TCDDTs from all transplants and found that spermatogenesis happened in all tissues. Importantly, functional spermatids could be isolated from all TCDDTs. Using this approach and fluorescence-activated cell sorting (FACS), we systemically analyzed the role of *c-kit*⁺ cells in postnatal development of testis. We identified that a small population of cells (*c-kit*⁺:*CD140a*⁺:*F4/80*⁺), which express typical markers of macrophages, were critical for *in vivo* testicular reconstitution.

Results

Functional spermatogenesis established in all testicular cell-derived tissues (TCDDTs) from transplants without Matrigel Matrix (MGM). To establish the system of *de novo* morphogenesis of testis, we modified a protocol that was previously reported by Kita et al²⁰. Briefly, testes of 5.5–6.5 days old male mice (B6D2F1 background) were decapsulated and digested into single cells. The cell suspension mixed with (the group 2), as reported by Kita et al²⁰, or without (the group 1) same volume of Matrigel Matrix (MGM), with a final concentration of 1×10^7 cells/ml, was injected subcutaneously into the backs of nude mice. A total of 1×10^6 cells (100 μ l of cell suspension) were injected for each transplant. Three months later, we observed tissue formation from all grafted cells with or without MGM (5 and 8, respectively) (Supplementary Fig. 1a). Interestingly, the average weight of the TCDDTs formed from the group 2 was significantly higher than that from the group 1 (Supplementary Fig. 1b). Histological analyses indicated, however, the presence of seminiferous tubular-like structures in all tissues from the group 1 while only a few tubules existed in the group 2 (Fig. 1a). Immunostaining of GATA-1, *Cyp17* and α -smoothmuscle actin (SMA), specific markers for mature sertoli cells, Leydig cells and myoid cells respectively, showed that a large number of typical testicular cords existed in TCDDTs from the group 1 (Fig. 1b and supplementary Fig. 1c) while typical cords were rarely observed in TCDDTs from the group 2 (Fig. 1c and supplementary Fig. 1c).

To test whether these cords contain functional niche for SSCs, we performed immunostaining with antibody against the mouse vasa homologue (MVH), a specific marker for germ cells. We observed that vast amounts of germ cells presented in all TCDDTs from the group 1 (around 60% of cords contained MVH⁺ cells) while sporadic cords containing MVH⁺ cells (less than 5%) in one TCDDT from the group 2 (Fig. 1d and supplementary Fig. 1c). Next, we tested whether haploid cells could be produced in TCDDTs by analyzing the DNA content of the cells dissociated from TCDDTs^{23,24}. Surprisingly, according to flow analysis, around 7.8% \pm 4.9% of total living cells were haploid in TCDDTs of the group 1 (Fig. 1e left) while no haploid cells could be found in TCDDTs of the group 2. Most of haploid cells were round spermatids (RS) and some of them were elongated spermatids (Fig. 1e right). To assess the epigenetic feature of FACS-enriched spermatids, we performed bisulfite sequencing to analyze the methylation profile of one paternally imprinted gene, *H19*, and one maternally imprinted gene, *Snrpn*. As expected, differentially methylated region (DMR) of *H19* retained largely intact methylation and the DMR of the *Snrpn* was free of methylation (Fig. 1f), suggesting that TCDDT-derived spermatids maintained a

typical paternal imprinting status. To test the function of TCDDT-derived spermatids, we performed intracytoplasmic round spermatid injection (ROSI). Injected oocytes cleaved into 2-cell embryos at a rate of 94% (Table 1), similar to that in control ROSI experiments (92%) (Table 1). 22% of two-cell embryos developed to blastocyst stage *in vitro* (Fig. 1g left). After transplantation of two-cell embryos or blastocysts into oviducts or uteri of pseudopregnant females respectively, a total of 6 live pups were recovered by caesarean section (C section) at 19.5 days of gestation (Fig. 1g right).

Next, we analyzed the process of cell reorganization and tissue formation by dissection of TCDDTs at different days after transplantation of testicular cells. Histological and immunostaining examinations indicated that the number of mature sertoli cells, myoid cells, Leydig cells and germ cells gradually increased following TCDDT growing and complete organized cords and spermatogenesis could be observed by day 45 after transplantation (Supplementary Fig. 1d).

Taken together, these results show that, without mixing with MGM, testicular cells from postnatal testes can *de novo* reconstitute TCDDTs from all transplants in nude mice (referred as functional TCDDTs to distinguish them from those from group 2), implying that this system may be feasible for investigating the roles of different cells in postnatal development of testis.

The role of SSCs in TCDDT formation. SSCs are the only known stem cells in adult testis that maintain self-renewal and spermatogenesis²⁵. We next assessed the role of SSCs in TCDDT formation. For this purpose, the endogenous SSCs were largely removed from testicular cells according to two cell surface markers, *c-kit* and *CD9*. *C-kit* is a marker for differentiating spermatogonia¹⁴ and *CD9* is a common surface marker for murine germline cells²⁶. *C-kit* negative and *CD9* positive (*c-kit*⁻:*CD9*⁺) cells (P4 zone in Fig. 2a) presented enriched SSC population, demonstrated by highly expression of *Oct4*²⁷ and *Gfra1*²⁸ (Fig. 2b), another two SSC markers. After depletion of *c-kit*⁻:*CD9*⁺ cells, the rest of testicular cells (P6 zone in Fig. 2a) were injected subcutaneously into the backs of nude mice at a concentration of 1×10^7 cells/ml (100 μ l of cell suspension per injection). We examined TCDDT formation three months later and found that all grafts formed tissues (9 of 9) (Supplementary Fig. 2a). The TCDDT from P6 zone cells had smaller size and lower weight than those of control TCDDTs (Supplementary Fig. 2b). Immunostaining analysis showed that typical testicular cords existed in all TCDDTs from P6 zone cells (Fig. 2c); however, germ cells could rarely be observed in these cords (Fig. 2d).

Next, we tested whether addition of exogenous SSCs in P6 zone cells could reestablish spermatogenesis in TCDDTs. To this end, we first generated SSC line by *in vitro* culturing *c-kit*⁻:*CD9*⁺ cells isolated from testes of *actin-EGFP* transgenic male mice (heterozygote) according to the protocol described by Kanatsu-Shinohara et al²⁹. The established SSC line (termed EGFP-SSC) showed typical SSC morphology (Supplementary Fig. 3a, b) and maintained paternal genomic imprints (Supplementary Fig. 3c). Moreover, EGFP-SSCs could restore spermatogenesis after transplantation into the testes of busulfan-treated male mice (Supplementary Fig. 3d), resulting in generation of functional male gametes (Supplementary Fig. 3e and Table 1). We then mixed the EGFP-SSCs with wide-type (WT) P6 zone cells at a ratio of 1:1 and transplanted into the backs of nude mice. Functional TCDDTs were formed from all grafts (3 of 3) and the weight of TCDDTs was resumed and even higher than that of control TCDDTs, probably due to the higher ratio of SSCs in injected cells than that in control cells (Supplementary Fig. 2a, b). Importantly, the EGFP-SSC recolonized in seminiferous cords derived from WT P6 zone cells and generated EGFP-SSC-derived spermatogenesis (Fig. 2e, f). Flow analysis indicated that TCDDTs contained around 5.5% of haploid cells, 41.6% of which were EGFP positive (Supplementary Fig. 2c), reflecting the donor SSCs carried heterozygous *EGFP* transgene. ROSI examinations demonstrated that spermatids

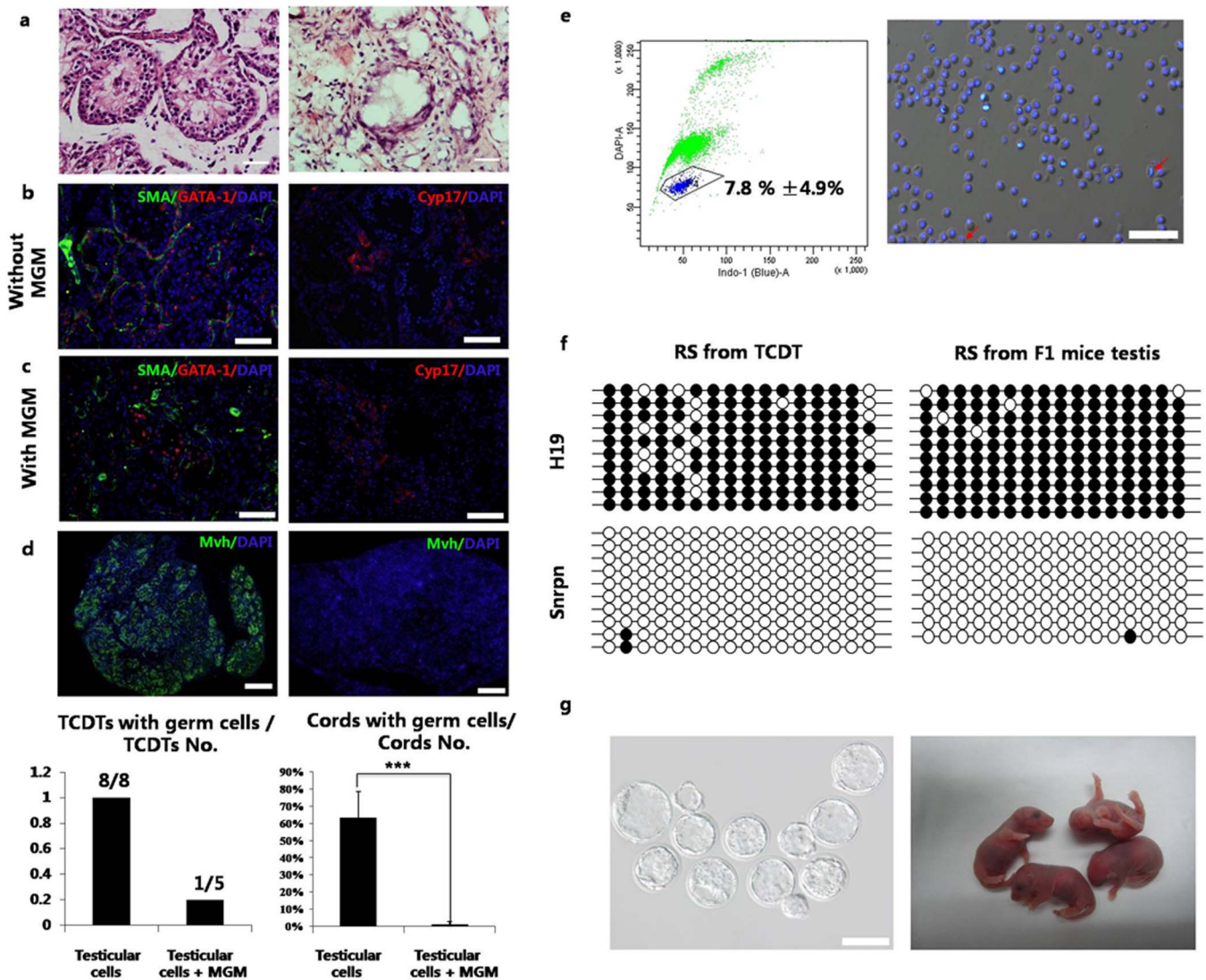


Figure 1 | *De novo* morphogenesis of testis by injection of neonatal testicular cells with or without Matrigel Matrix (MGM) (group 2 and group 1, respectively) into nude mice. (a) Histochemical analysis of TCDTs from the group 1 (left) and group 2 (right) respectively. Typical seminiferous tubular-like structures exist in TCDT of group 1, termed functional TCDT, but not in TCDT of group 2. Scale bar, 50 μm . (b) Immunostaining of GATA 1, Cyp17 and α -smooth muscle actin (SMA) in one cryosection of TCDT from group 1. Typical testicular cords exist in TCDTs from group 1. Nuclei were stained with DAPI (blue fluorescence). Scale bar, 50 μm . (c) Immunostaining images of one cryosection of TCDT from group 2. Typical cords were rarely observed in TCDTs from group 2. Scale bar, 50 μm . (d) Immunostaining with antibody against MVH. Upper, immunostaining images of cryosections of TCDTs from group 1 (left) and group 2 (right) respectively. Bottom, vast amounts of germ cells presented in all TCDTs from group 1 (around 60% of cords contained MVH⁺ cells ($n = 3$)) while sporadic cords containing MVH⁺ cells (less than 5%) in one TCDT from group 2 ($n = 4$). Scale bar, 500 μm . Values are means \pm SD, *** $P < 0.001$. (e) Flow analysis of functional TCDTs from group 1. Left, around 7.8% of total living cells are haploid in TCDTs of group 1 ($n = 6$). Right, most of haploid cells are round spermatids (RS), while some of them are elongated spermatids (red arrows). Values are means \pm SD. Scale bar, 50 μm . (f) Bisulfite sequencing analysis of RS from functional TCDTs. Upper, the differentially methylated region (DMR) of *H19* retains largely intact methylation in RS from TCDT of group 1 (left). Bottom, the DMR of the *Snrpn* is free of methylation in RS from TCDT of group 1 (left). Open and filled circles represent unmethylated and methylated CpG sites, respectively. (g) Images of embryos derived after injection of RS from TCDT of group 1 into oocytes, showing that they could support *in vitro* (blastocyst stage, left) and *in vivo* development (newborn pups, right) after injection into oocytes. Scale bar, 50 μm .

isolated from TCDTs were competent for fertilization to produce the progeny (Fig. 2g and Table 1). Taken together, these data validates the idea that the system of *de novo* morphogenesis of testis is feasible for analyzing the function of different cells in postnatal development of testis.

Interstitial *c-kit*⁺ cells (*c-kit*⁺:CD140a⁺ cells) are critical for the TCDT formation. We next investigated the role of *c-kit*⁺ cells in TCDT formation. As shown in Fig. 3a, around 3.8% of testicular cells dissociated from testes of 6.5 days old mice (WT mice, Fig. 3a left and

EGFP mice, Fig. 3a right) were *c-kit*⁺ cells. After transplantation of *c-kit*⁺ cells into nude mice, only 2 of 20 grafts formed TCDTs with very small size, indicating that *c-kit*⁺ cells were critical for TCDT formation (Fig. 3b, c). To further verify the vital role of *c-kit*⁺ cells in TCDT formation, *c-kit*⁺ cells from EGFP-marked testes were mixed with *c-kit*⁻ cells from WT mice (B6D2F1) for subcutaneous injection (Fig. 3a). As expected, all three grafts formed TCDTs with similar size to control TCDTs (Fig. 3b, c). Immunostaining analysis demonstrated that seminiferous cords and spermatogenesis existed in all three TCDTs (Fig. 3d). Interestingly, most EGFP positive cells



Table 1 | Summary of ROSI experiments

Origin of injected RS*	No. of Injected oocytes	No. of 2-cell	Embryo Stage	No. of Embryos Transferred	No. of recipients	Number of Pups (% of Transferred Embryos)	Number of Pups Surviving to Adulthood
TCDTs from F1 mice	86	72	Blastocyst	16	1	2 (12.5)	1
	150	150	two-cell	60	2	4 (6.7)	4
EGFP-SSCs Reconstituted testes	62	58	blastocyst	12	1	4 (33.3)	3
TCDTs from P6 zone cells plus EGFP-SSCs	114	112	blastocyst	36	2	5 (13.8)	4
C-Kit ⁺ EGFP-SSCs Reconstituted testes	135	134	two-cell	60	2	6 (10)	6
TCDTs from F1 c-Kit ⁻ plus EGFP c-kit ⁺ :CD140a ⁺ cells	68	60	two-cell	40	2	5 (12.5)	2
TCDTs from F1 c-Kit ⁻ plus EGFP F4/80 ⁺ cells	120	105	two-cell	75	3	13 (17.3)	13
F1 mice	52	48	blastocyst	12	1	3 (25)	3

*: RS, round spermatids.

located in interstitium of TCDTs and didn't express Cyp17 (Fig. 3d); while a small number of EGFP⁺ cells were observed in seminiferous cords and expressed MVH (Fig. 3e). Because c-kit⁺ cells could be roughly divided into two fractions according to their light-scattering features (Supplementary Fig. 4a), we proposed that two subpopulations of c-kit⁺ cells, which produced progeny cells distribution in

interstitium and seminiferous cords respectively, exist in postnatal testes.

We attempted to separate c-kit⁺ cells into two subpopulations on the basis of surface markers. Flow analyses showed that CD140a could separate c-kit⁺ cells into two groups (Fig. 4a and Supplementary Fig. 4b, c). Immunostaining analysis of postnatal testis

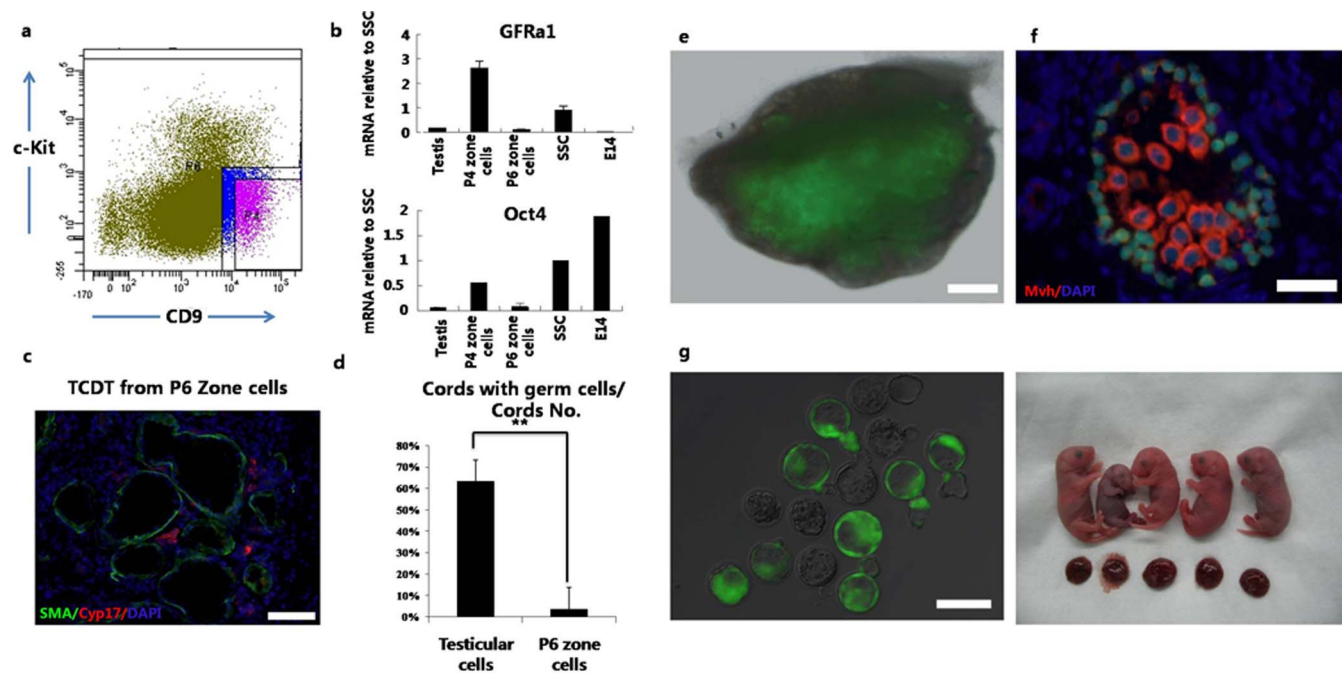


Figure 2 | The role of SSCs in TCDT formation. (a) C-kit negative and CD9 positive (c-kit⁻:CD9⁺) cells were enriched from testicular cells of neonatal mice via FACS. C-kit negative and CD9 positive (c-kit⁻:CD9⁺) cells (P4 zone) presented enriched SSC population. (b) C-kit⁻:CD9⁺ cells (P4 zone cells) highly expressed Oct4 and GFRa1, another two SSC markers. The expression levels were relative to those in established SSC line, which were set to 1. Results were from three independent cell sorting. Values are means ± SD. (c) Immunostaining analysis of TCDT formed from P6 zone cells (testicular cells without P4 zone cells). Typical testicular cords, which contain a large amount of Cyp17 positive cells (red fluorescence) and SMA positive cells (green fluorescence), exist in all TCDTs from P6 zone cells. The nuclei were stained with DAPI (blue fluorescence). Scale bar, 50 μm. (d) Summary of the ratio of cords with germ cells in total cords in TCDTs formed from testicular cells (n = 3) and P6 zone cells (n = 5). Germ cells can be rarely observed in the cords of TCDTs formed from P6 zone cells. Values are means ± SD, ** 0.001 < P < 0.01. (e) Image of the TCDT formed from WT P6 zone cells plus exogenous EGFP-marked SSCs. EGFP-positive cells can be observed in entire TCDT. Scale bar, 2 mm. (f) Immunostaining analysis of TCDT formed from WT P6 zone cells plus exogenous EGFP-marked SSCs. All EGFP positive cells express Mvh, indicating that EGFP-SSCs recolonize in seminiferous cords derived from WT P6 zone cells and generate EGFP-SSC-derived spermatogenesis. The nuclei were stained with DAPI. Scale bar, 50 μm. (g) FACS-enriched haploid cells could support *in vitro* and *in vivo* development after injection into oocytes (ROSI). Left, blastocysts generated from ROSI experiments. Some of them are EGFP positive, reflecting that donor SSCs carried heterozygous EGFP transgene. Right, the newborn pups from ROSI experiments. Scale bar, 100 μm.

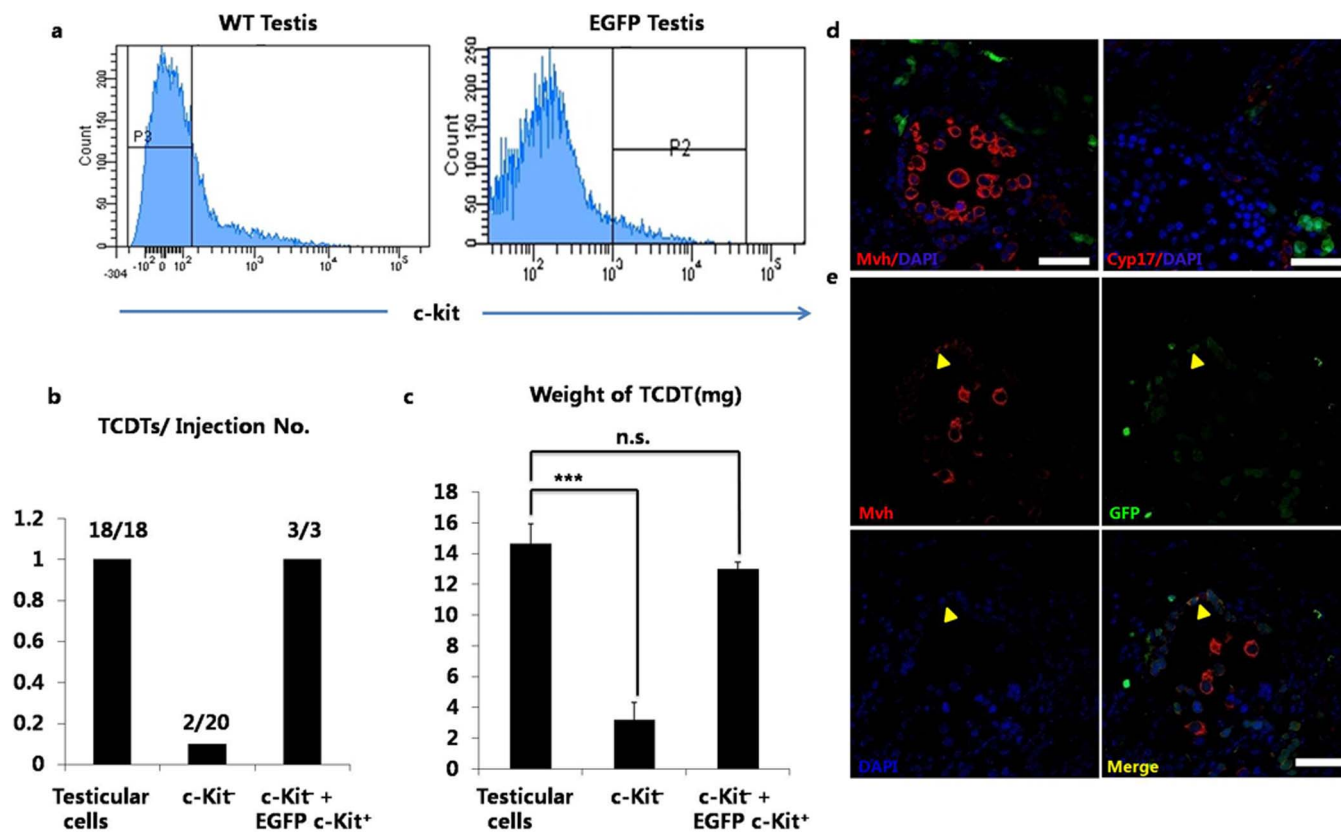


Figure 3 | The role of $c\text{-kit}^+$ cells in TCDT formation. (a) WT $c\text{-kit}^-$ cells (P3 zone cells in left picture) plus EGFP- $c\text{-kit}^+$ cells (P2 zone cells) were injected into nude mice for TCDT formation. (b) Summary of TCDT formation. After depletion of $c\text{-kit}^+$ cells from testicular cells of neonatal testes, only 2 of 20 grafts of $c\text{-kit}^-$ cells formed TCDTs. After reimbursement of EGFP- $c\text{-kit}^+$ cells from neonatal testes into WT $c\text{-kit}^-$ cells, all 3 grafts formed TCDTs. (c) The weight of TCDTs. TCDT from $c\text{-kit}^-$ cells had a smaller size than controls. After reimbursement of EGFP- $c\text{-kit}^+$ cells, TCDT could be formed with similar size to control TCDTs ($n = 5, 2$ and 3 for each group, respectively). Values are means \pm SD. “n.s.” means no significant difference, *** $P = 0.0001$. (d) Immunostaining of Mvh and Cyp17 in sections of TCDTs from the group of WT $c\text{-kit}^-$ cells plus EGFP- $c\text{-kit}^+$ cells. Most EGFP positive cells located in interstitium of TCDTs and didn’t express Cyp17. Scale bar, 50 μm . (e) Immunostaining of the same section as (d). Yellow arrowheads indicate that there are a small number of EGFP⁺ cells in seminiferous cords, which express MVH. Scale bar, 50 μm .

indicated that, consistent with previous observations^{16,30}, CD140a (also known as platelet-derived growth factor α , *PDGFR*) was specifically expressed in interstitial cells and $c\text{-kit}$ was expressed both in the seminiferous and interstitial cells (Fig. 4b). Furthermore, FACS-enriched $c\text{-kit}^+:\text{CD140a}^-$ cells, but not $c\text{-kit}^+:\text{CD140a}^+$ cells, expressed MVH (Fig. 4c) and also CD49f (also known as integrin $\alpha 6$)¹⁸ (Supplementary Fig. 4d), another well-known surface marker for mouse germ cell. Finally, *in vitro* culture experiments showed that $c\text{-kit}^+:\text{CD140a}^+$ cells did not expand in SSC culture environment (Supplementary Fig. 4e, left). In contrast, some $c\text{-kit}^+:\text{CD140a}^-$ cells proliferated (Supplementary Fig. 4e, right) and formed a functional SSC line (termed $c\text{-kit}^+ \text{-EGFP-SSC}$) (Supplementary Fig. 5a–d). This is consistent with a previous report that differentiating SSCs can be converted into undifferentiating state *in vitro* and *in vivo*³¹, supporting our early observations that a small amount of EGFP-marked $c\text{-kit}^+$ cells recolonized in seminiferous tubules of TCDTs (Fig. 3e). Taken together, $c\text{-kit}^+$ is expressed both in interstitial and seminiferous cells and CD140a is a suitable surface marker for distinguishing two subpopulations of $c\text{-kit}^+$ cells.

We next tested the roles of interstitial and seminiferous $c\text{-kit}^+$ cells in TCDT formation. After injection of cell suspensions containing WT $c\text{-kit}^-$ cells and EGFP-marked $c\text{-kit}^+:\text{CD140a}^+$ cells into nude mice, all transplants (7 of 7) formed TCDTs with comparable weight to controls three months later (Fig. 4d). In contrast, $c\text{-kit}^+:\text{CD140a}^-$ cells did not rescue the failure of TCDT formation induced by $c\text{-kit}^+$ cells depletion (3 of 6 formed TCDTs with small size, Fig. 4d). We found that integral seminiferous cords and spermatogenesis existed

in all TCDTs derived after reimbursement of exogenous $c\text{-kit}^+:\text{CD140a}^+$ cells in $c\text{-kit}^-$ cells (Fig. 4e). Haploid cells (Fig. 4f) were enriched by FACS and competent for fertilization (Fig. 4g and Table 1). Together, interstitial $c\text{-kit}^+:\text{CD140a}^+$ cells alone can rescue the failure of TCDT formation induced by depletion of $c\text{-kit}^+$ cells from testicular cells.

A small subpopulation of interstitial $c\text{-kit}^+:\text{CD140a}^+:\text{F4/80}^+$ cells determine the TCDT formation. The constitutively expressed EGFP in donor cells provides a system for lineage tracing of individual cell population in TCDT formation. Green-fluorescence cells, which were the progeny cells of EGFP-marked $c\text{-kit}^+:\text{CD140a}^+$ cells were all located in interstitium (Fig. 4e). Interestingly, these cells didn’t express Cyp17 (Fig. 4e), consistent with our early observations in Fig. 3d, indicating that $c\text{-kit}^+:\text{CD140a}^+$ cells do not include the progenitor cells of adult Leydig cells. Because Leydig cell is the only known interstitial cell that expresses $c\text{-kit}$ by now^{13–15,32}, these results imply that different types of $c\text{-kit}^+$ cells exist in interstitium and play important role in TCDT formation. To test this hypothesis, we enriched $c\text{-kit}^+:\text{CD140a}^+$ cells of testis from 6.5 days old mice by FACS. Immunostaining analysis showed that around 50% of $c\text{-kit}^+:\text{CD140a}^+$ cells expressed Cyp17 (Fig. 5a). Because progeny cells of exogenous $c\text{-kit}^+:\text{CD140a}^+$ cells in TCDTs didn’t express Cyp17 (Fig. 3d and Fig. 4e), we concluded that these $c\text{-kit}^+:\text{CD140a}^+:\text{Cyp17}^+$ cells were fetal Leydig cells, which persisted in postnatal interstitium and were eventually replaced by adult Leydig cells in TCDT, consistent with the observations in normal testicular development³³.

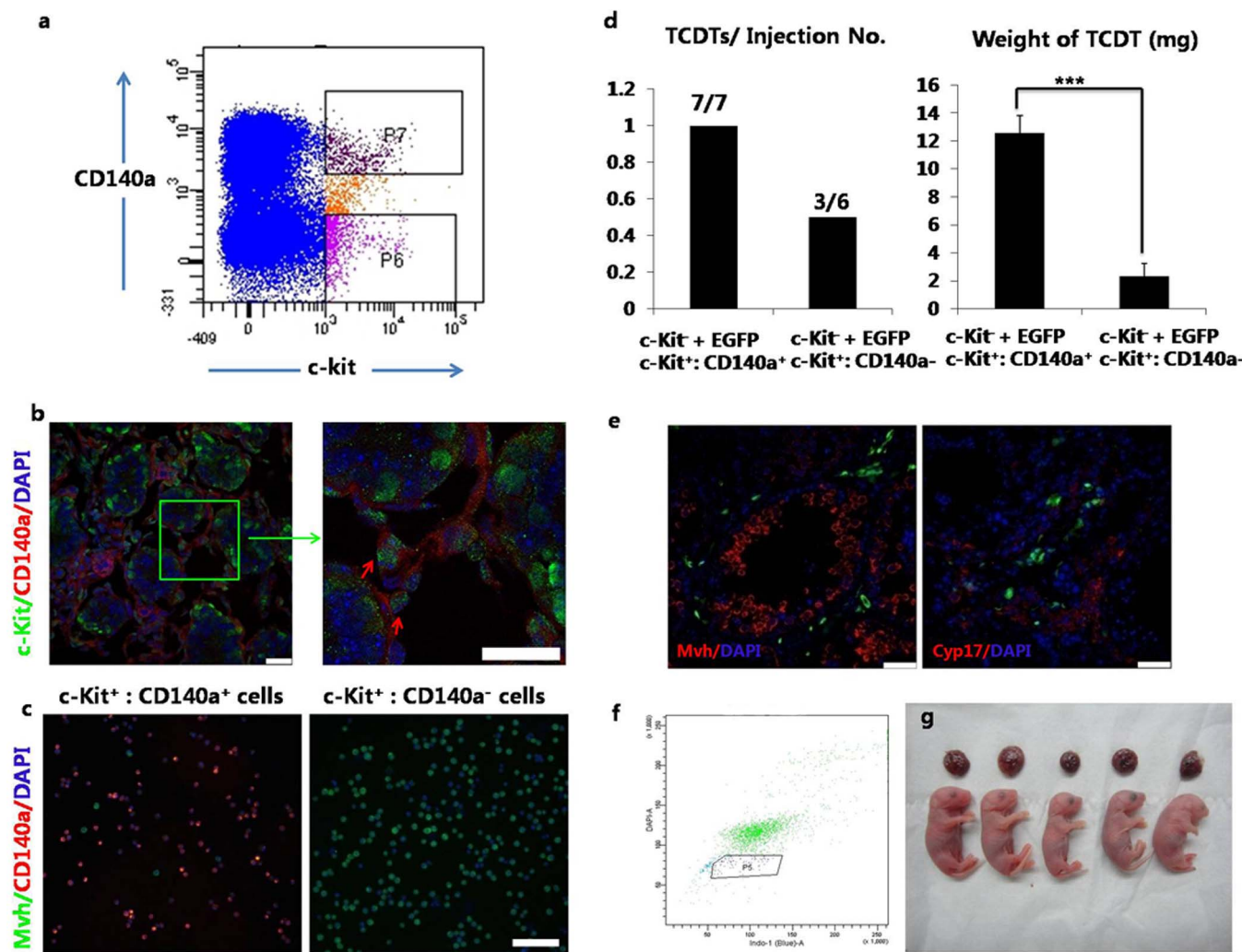


Figure 4 | Interstitial c-kit⁺ (c-kit⁺:CD140a⁺) cells are critical for the TCDT formation. (a) Flow analysis showed that CD140a could separate c-kit⁺ cells of neonatal testes into two groups (P6 zone and P7 zone). (b) Immunostaining analysis of postnatal testis indicated that CD140a (red fluorescence) was specifically expressed in interstitial cells and c-kit (green fluorescence) was expressed both in the seminiferous and interstitial cells. Green box in left image is magnified in right. Scale bars, 25 μ m. (c) Immunostaining of FACS-enriched c-kit⁺:CD140a⁻ cells and c-kit⁺:CD140a⁺ cells using CD140a and Mvh antibodies. Left, c-kit⁺:CD140a⁺ cells don't express Mvh. Right, c-kit⁺:CD140a⁻ cells express Mvh. Scale bar, 50 μ m. (d) Summary of TCDT formation. Left, interstitial c-kit⁺ (EGFP-marked c-kit⁺:CD140a⁺) cells alone (n = 7), but not c-kit⁺:CD140a⁻ cells (EGFP marked) (n = 6), could rescue the failure of TCDT formation induced by c-kit⁺ cell depletion. Right, the average weight of TCDTs (n = 4) formed from c-kit⁺ cells plus exogenous c-kit⁺:CD140a⁺ cells were significantly higher than that of TCDTs (n = 3) from c-kit⁺ cells plus exogenous c-kit⁺:CD140a⁻ cells. Values are means \pm SD, *** P < 0.001. (e) Immunostaining analysis of TCDT from the group of WT c-kit⁺ cells plus EGFP-marked c-kit⁺:CD140a⁺ cells using Mvh and Cyp17 antibodies. Integral seminiferous cords and spermatogenesis exist in the TCDTs, indicating that these are functional TCDTs. EGFP positive cells, which are progeny cell of donor c-kit⁺:CD140a⁺ cells, locate in interstitium and don't express Cyp17, reflecting that c-kit⁺:CD140a⁺ cells are not progenitors of Leydig cells. Scale bars, 50 μ m. (f) Haploid cells could be enriched from TCDTs formed from WT c-kit⁺ cells plus EGFP-marked c-kit⁺:CD140a⁺ cells through FACS. (g) Newborn pups developed from reconstituted oocytes after injection of haploid cells enriched from TCDT showed in (f).

We next attempted to identify what the c-kit⁺:CD140a⁺:Cyp17⁻ cells are. It is well known that macrophages comprise a substantial portion of interstitial cells of testis^{34,35}. We then performed flow analysis according to F4/80, a surface marker of macrophages^{36,37}. As expected, we found around 0.35% of testicular cells from 6.5 days old pups were F4/80 positive cells and all these cells expressed c-kit (Fig. 5b). Furthermore, c-kit⁺:CD140a⁺ cells could be divided into two subpopulations according to F4/80 antibody (Fig. 5c). Flow analysis showed that all the F4/80 positive cells in the neonatal testes were also CD11b positive, another well-known surface marker of macrophage³⁸. Furthermore, real-time PCR analysis showed that c-kit⁺:CD140a⁺:F4/80⁺ (termed F4/80⁺ cells) highly expressed transforming growth factor- β (*TGF β*)^{39,40}, a secretory protein of testicular macrophages, while c-kit⁺:CD140a⁺:F4/80⁻ cells (termed F4/

80⁻ cells) expressed *Cyp17* and *3 β HSD*, specific markers for adult Leydig cells⁴¹ (Supplementary Fig. 6a). *In vitro* culturing experiments showed that F4/80⁺ cells could expand in Macrophage Complete Medium (MCM)³⁸ (Supplementary Fig. 6b), but could not in a standard culture medium for mouse embryonic fibroblasts (MEF). By contrast, F4/80⁻ cells could be maintained in MEF medium (Supplementary Fig. 6c). Functional analyses showed that F4/80⁺ cells inhibited the proliferation of T cells (Supplementary Fig. 6d)⁴² and promoted the testosterone secretion by F4/80⁻ cells *in vitro* (Supplementary Fig. 6e)⁴³. Taken together, these data demonstrate that F4/80⁺ cells are most likely macrophages and F4/80⁻ cells mostly comprise fetal Leydig cells.

We then analyzed the roles of F4/80⁺ and F4/80⁻ cells in TCDT formation. After injection of cell suspensions containing WT c-kit⁺

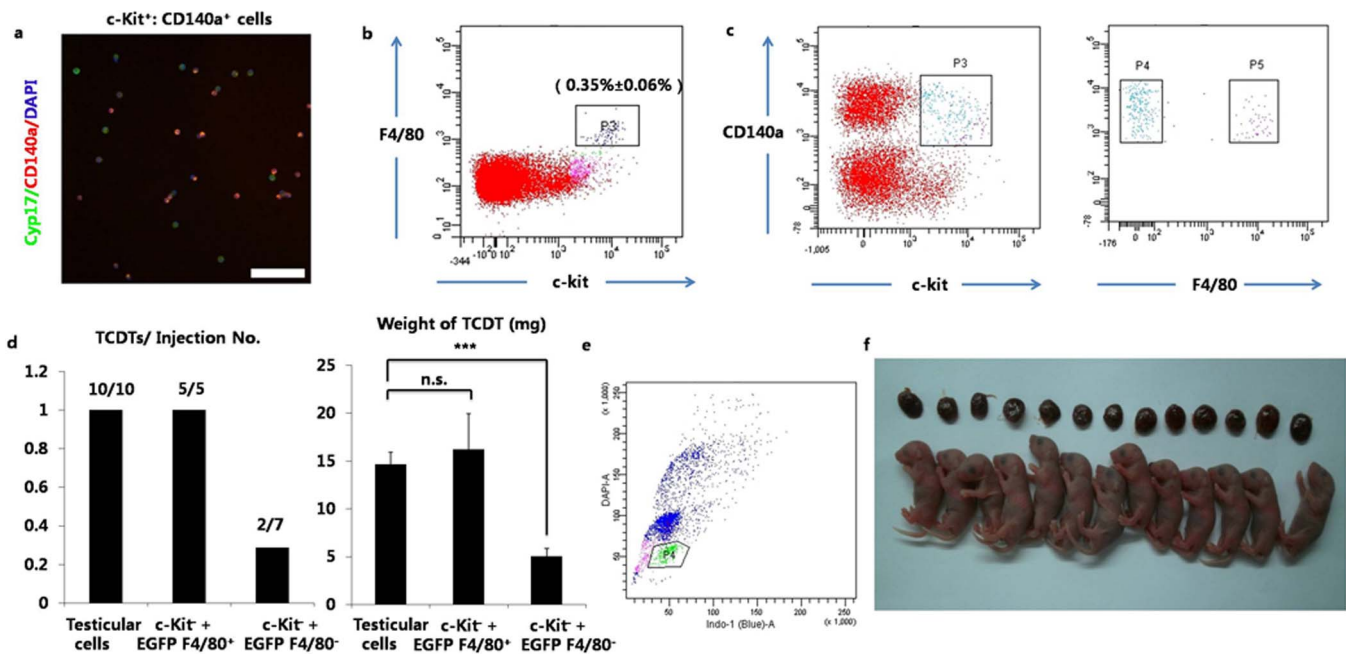


Figure 5 | A small subpopulation of interstitial $c\text{-kit}^+$ cells ($c\text{-kit}^+:\text{CD140a}^+:\text{F4/80}^+$ cells, termed F4/80^+ cells) determine the TCDT formation. (a) Immunostaining analysis of $c\text{-kit}^+:\text{CD140a}^+$ cells FNACS-enriched from neonatal testes using CD140a and Cyp17 antibodies. Around 50% of $c\text{-kit}^+:\text{CD140a}^+$ cells express Cyp17, implying that $c\text{-kit}^+:\text{CD140a}^+:\text{Cyp17}^+$ cells are fetal Leydig cells. Scale bar, 50 μm . (b) Flow analysis of testicular cells from 6.5 days old pups using F4/80 and $c\text{-kit}$ antibodies. Around 0.35% of testicular cells are F4/80 positive cells and all these cells expressed $c\text{-kit}$ ($n = 5$). Values are means \pm SD. (c) Flow analysis of $c\text{-kit}^+:\text{CD140a}^+$ cells using F4/80 antibody. $c\text{-kit}^+:\text{CD140a}^+$ cells of testicular cells (left) can be divided into two subpopulations according to F4/80 antibody (right). (d) Summary of TCDT formation. Left, F4/80^+ cells (EGFP-marked) alone can rescue the failure of TCDT formation induced by $c\text{-kit}^+$ cells depletion ($n = 5$), while F4/80^- cells alone cannot (only 2 of 7 formed TCDTs). Right, the average weight of TCDTs ($n = 4$) formed from $c\text{-kit}^-$ cells plus exogenous EGFP-marked F4/80^+ cells is significantly higher than that of TCDTs ($n = 2$) from $c\text{-kit}^-$ cells plus exogenous F4/80^- cells, but comparable to that of control TCDTs ($n = 5$). Values are means \pm SD. “n.s.” means no significant difference, *** $P < 0.001$. (e) Haploid cells could be enriched from TCDTs of $c\text{-kit}^-$ cells plus EGFP-marked F4/80^+ cells, indicating these were functional TCDTs. (f) Newborn pups developed from reconstituted oocytes after injection of haploid cells enriched from TCDT showed in (e).

cells (one million cells) and EGFP-marked F4/80^+ cells (25 thousands cells) into nude mice, all transplants (5 of 5) formed TCDTs with comparable weight to controls three months later (Fig. 5d). In contrast, F4/80^- cells did not rescue the failure of TCDT formation induced by $c\text{-kit}^+$ cells depletion (2 of 7 formed TCDTs with small size, Fig. 5d). Haploid cells (Fig. 5e) could be enriched from TCDTs and support full-term development of injected oocytes (Fig. 5f and Table 1). Together, F4/80^+ cells alone can rescue the failure of TCDT formation induced by depletion of $c\text{-kit}^+$ cells from testicular cells.

F4/80^+ cells are gradually replaced by cells from recipient mice during TCDT formation. Next, we analyzed the distribution of EGFP-positive cells, which were the progeny cells of EGFP-marked F4/80^+ cells from fetal testes. Surprisingly, no EGFP-positive cells could be observed in all TCDTs (Fig. 6a, b), while a significant population of F4/80^+ cells existed in all TCDTs (Fig. 6b). To test the origin of TCDT-derived F4/80^+ cells, DNA was extracted and employed for simple sequence-length polymorphism (SSLP). The results showed that the TCDT-derived F4/80^+ cells had a polymorphic pattern same as that of recipient strain (BALB/C), but different from the strain of injected cells isolated from neonatal testes (B6D2F1, Fig. 6c). *In vitro* culturing experiments showed that TCDT-derived F4/80^+ cells could expand in MCM (Fig. 6d), but could not in a standard culture medium for MEF. Functional analyses showed that TCDT-derived F4/80^+ cells could inhibit the proliferation of T cells (Fig. 6e), indicating that TCDT-derived F4/80^+ cells, which were originate from peripheral blood of recipient mice, were most likely macrophages. We then analyzed the timing of F4/80^+ cells replacement during TCDT formation by dissecting TCDT at 30, 45, 60 days post injection of EGFP-marked

testicular cells into nude mice. Cells were dissociated from TCDTs and employed for flow analysis. The results showed that the ratio of total F4/80^+ cells gradually increased while EGFP-marked F4/80^+ cells gradually reduced (Fig. 6f).

Finally, we investigated whether F4/80^+ cells from other sources, including F4/80^+ cells from adult testes, peritoneal F4/80^+ cells and bone-marrow-cell-derived F4/80^+ cells, can be used in place of F4/80^+ cells from neonatal testes to rescue the failure of TCDT formation induced by $c\text{-kit}^+$ cells depletion. To this end, 25 thousands of F4/80^+ cells were mixed with 1 million $c\text{-kit}^-$ testicular cells from neonatal mice for each transplantation. Three month later, we didn't find the TCDT formation from all injection sites (4 from F4/80^+ cells from adult testes, 4 from peritoneal F4/80^+ cells and 3 from bone-marrow-cell-derived F4/80^+ cells).

Taken together, $c\text{-kit}^+:\text{CD140a}^+:\text{F4/80}^+$ cells from fetal testes are critical for TCDT formation; however, these cells are gradually eliminated and replaced by F4/80^+ cells originated from peripheral blood cells of recipient mice.

Discussion

The mammalian testis is complex organ and provides a host to spermatogenesis, one of the most intricate cell divisions occurring in postnatal life. Different cells participate in testicular development and play different roles in spermatogenesis. Great efforts have been made and a variety of model systems have been established since early in 20th century to recapitulate the spermatogenesis *in vitro* and *in vivo*^{19,44,45}. However, none of these systems are feasible for analyzing cellular function in postnatal testicular development and spermatogenesis. *De novo* morphogenesis of testis^{19–21}, a developing technique, provides a unique method to study testicular development

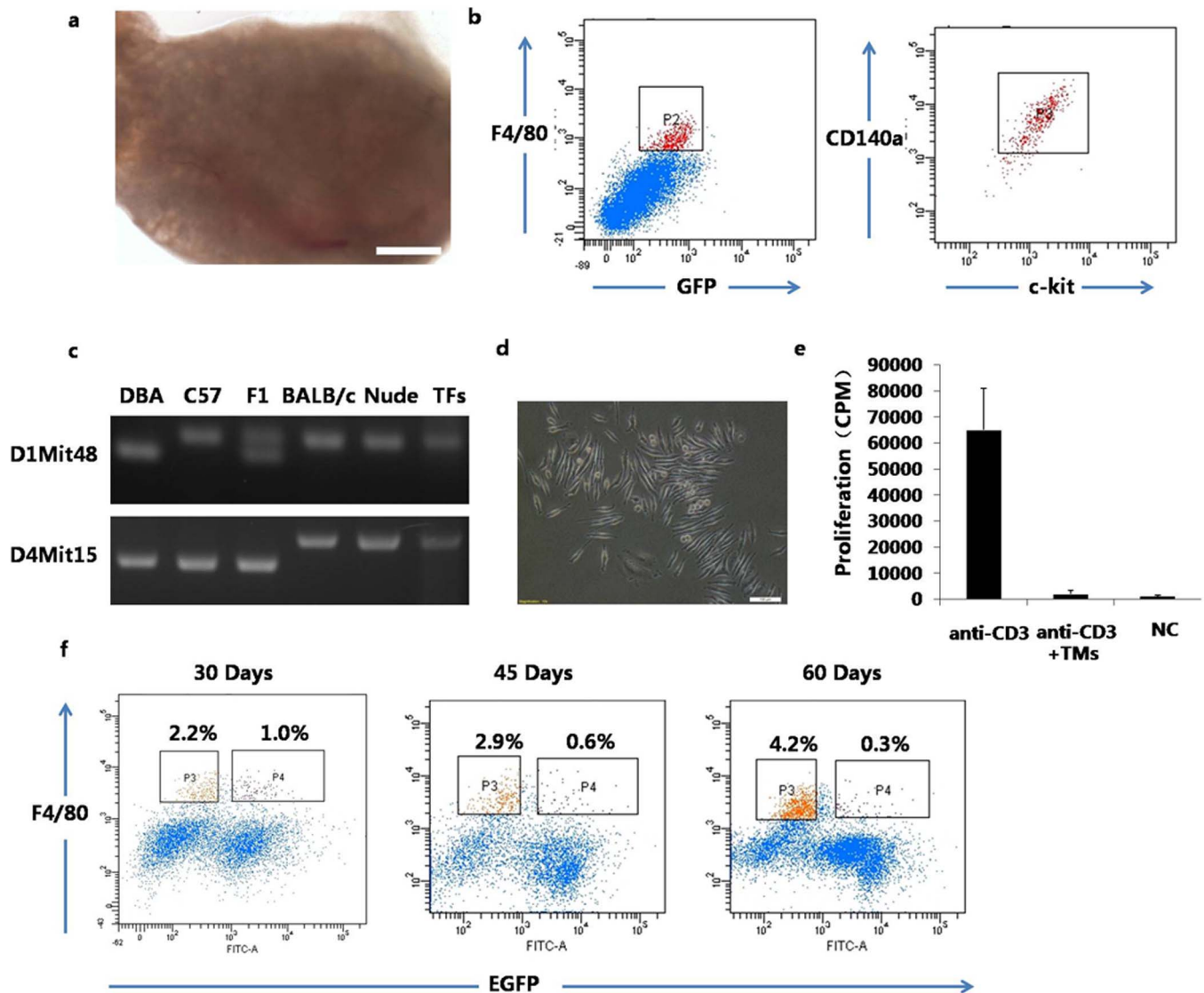


Figure 6 | C-kit⁺;CD140a⁺;F4/80⁺ cells from neonatal mice are gradually replaced by circulating cells during TCDT formation. (a) Fluorescent image of one TCDT formed from c-kit⁻ cells plus EGFP-marked c-kit⁺;CD140a⁺;F4/80⁺ cells. No EGFP positive cells can be detected (n = 5). Scale bar, 500 μ m. (b) Flow analysis of cells isolated from TCDTs using c-kit, CD140a and F4/80 antibodies. Left, no EGFP-positive cells exist in all TCDTs, but a substantial amount of F4/80⁺ cells exist. Right, F4/80⁺ cells are CD140a and c-kit double positive cells. (c) Simple sequence-length polymorphism (SSLP) analysis of F4/80⁺ cells enriched from formed TCDTs. F4/80⁺ cells in TCDTs have a polymorphic pattern same as that of recipient strain (nude mice, BALB/C strain), but different from the strain (F1) of injected F4/80⁺ cells from neonatal testes. TFs, TCDT-derived F4/80⁺ cells. (d) *In vitro* culture of TFs showed that these cells could proliferate in MCM, a medium used for *in vitro* of macrophages. (e) TFs could inhibit the proliferation of T cells. Anti-CD3 antibody could activate the splenocyte proliferation, while TFs greatly suppressed the proliferation of splenocytes activated by anti-CD3 antibody. Results were from three independent experiments. Values are means \pm SD. (f) Flow analysis of the ratio of F4/80⁺ cells during TCDT growing from EGFP-testicular cells from neonatal mice. TFs from neonatal testes (EGFP positive cells) were gradually eliminated and replaced by peripheral blood cells (EGFP⁻;F4/80⁺ cells) of recipient mice during TCDT growing.

since it enables to manipulate various cells prior to grafting⁴⁶. However, this application has not yet been tested experimentally. Moreover, the system reported to date shows very low spermatogenesis^{20,21} in reconstituted tissues, greatly restricting its application. In our study, we modified the system by removing MGM from reported protocol²⁰ and injecting freshly isolated testicular cells into nude mice. We found that TCDTs were generated from all grafts (48 of 48). Surprisingly, functional spermatogenesis occurred in all TCDTs (48 of 48) and the highest ratio of haploid cells in total cells of TCDT was 13.3%. MGM has been used for 3-Dimensional culture of immature testicular cells to support cord formation^{47,48} and later for *in vivo* morphogenesis of testis²⁰. Although MGM may help testis-like tissue formation *in vitro* and *in vivo*, consistent with significantly higher

weight of TCDTs from the group 2 with MGM than that from the group 1 without MGM in this study (Supplementary Fig. 1a), MGM may not be benefit for homing of SSC, resulting in low spermatogenesis in formed tissues as shown in this study (Fig. 1d) and reported previously²⁰.

We develop a new strategy for studying the function of different cells in testicular development by employing the technical combination of cell sorting and *de novo* morphogenesis of testis. In this system, interested cells in testes are removed and reimbursed with same cells carrying transgene of fluorescent proteins, such as EGFP (Fig. 7a). The reconstituted cell suspensions are used for TCDT formation and the fluorescence-marked cells can be traced in formed tissues. We validate this system by depleting endogenous SSCs and



addition of exogenous SSCs carrying EGFP transgene (Fig. 2). We further systemically analyze the roles of *c-kit*⁺ cells in TCDT formation and identify that a small population of *c-kit*⁺ cells (*c-kit*⁺:*CD140a*⁺:*F4/80*⁺ cells) (Fig. 7b) from neonatal mice, which are most likely testicular macrophages, play critical role in TCDT formation.

Macrophages are important accessory cells for testicular development and decide the testis as one ‘immunological privileged’ tissue of the body^{34,35,49}. However, there is no direct evidence that macrophages are critical for testicular development because all reports to date are based on depletion of macrophages by chemical treatment^{50,51} or gene knockout⁵² experiments, in which, macrophages can not be completely removed from testes. Meanwhile, it is still not clear the origin of testicular macrophages⁵³. One possibility of their origination is that cells from blood move into testis and locally differentiate into macrophages⁵⁵; however, this hypothesis has not been proven yet. Here, we provide the most direct evidence to date that *c-kit*⁺:*CD140a*⁺:*F4/80*⁺ cells of neonatal testis, which are most likely macrophages, are critical for testicular development and *F4/80*⁺ cells of adult testes are most likely derived from peripheral blood cells.

In summary, we have shown several advantages of this new strategy in our study (i) the function of specific type of cells in testicular development can be demonstrated by deletion of these cells from testicular cells for TCDT formation and further confirmed by restoration-of-function experiments, i.e., reimbursement of the same type of cells to the rest of testicular cells; (ii) addition of exogenous cells carrying transgenes provides an opportunity to trace the progeny cells of donor cells in formed TCDTs, allowing us to reveal new progenitor cells of specific cell type, such as adult Leydig stem cells; and (iii) genetic modification in a specific type of cells *in vitro* before

TCDT formation allows us to elucidate the gene function in testicular development and spermatogenesis.

Methods

Animal use and care. All animal procedures were carried out in accordance with the approved guidelines of the Institute of Biochemistry and Cell Biology, Shanghai Institutes for Biological Sciences, China.

WT B6D2F1 mice or EGFP-F1 mice were derived from WT or actin-EGFP C57BL/6 female mice after mating with DBA/2J male mice. Nude mouse were purchased from SLACS (Shanghai, China).

Generation of testicular cell-derived tissue (TCDT). Donor cells for transplantation were prepared from testes of WT F1 or EGFP-F1 mice (5.5–6.5 days old). The testes were decapsulated and were digested by a two-step enzymatic treatment. Briefly, testicular tissue was treated with digestion solution 1 containing collagenase type IV (1 mg/ml) and DNase (150 ug/ml) in DMEM at 37°C for 20 min. The specimens were centrifuged and washed twice with PBS and digested with trypsin at 37°C for 5 min. The cell suspension was filtered through mesh with a pore size of 40 μm. For subcutaneous injection, we counted the cell number using the Countess (Invitrogen). The cell suspension with or without MGM was injected subcutaneously using a 26-G needle into the dorsal region of the nude mice at 1×10^6 cells per site. Animals were randomly divided into several groups by a third person. Each animal was injected at one or two sites.

Preparation of *F4/80*⁺ cells from other sources. Peritoneal *F4/80*⁺ cells were prepared by intraperitoneal injection of 4% thioglycollate into B2D6F1 mice (8 wks). Three days later, elicited peritoneal *F4/80*⁺ cells were harvested by recovering the DMEM medium following injection them into the peritoneal cavity. To obtain bone-marrow-derived *F4/80*⁺ cells, bone marrow cells from femurs and tibias of B6D2F1 mice (8 wks) were cultured in DMEM/F12 medium supplemented with 10% FBS and 20 ng/ml M-CSF (eBioscience) for 7 days.

Cell sorting. The testicular cells were suspended with moderate PBS containing 8% fetal bovine serum (PBS/FBS) and were incubated with antibodies. Flow cytometric analyses were performed using a standard protocol. All the antibody information was listed in Table S1. Antibody incubations were performed on ice for 30 min and cells were washed with PBS/FBS twice. For sorted the haploid cell from the testes and

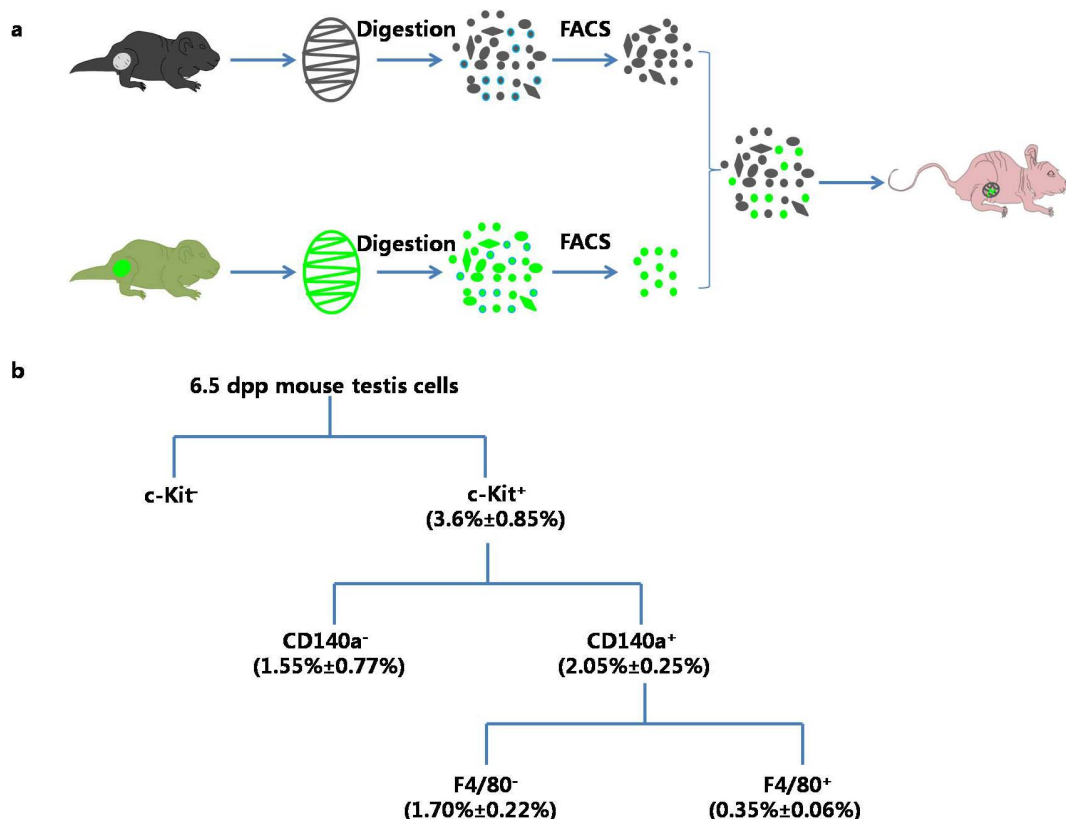


Figure 7 | The diagram and application of *de novo* morphogenesis of testis. (a) Diagram of *de novo* morphogenesis of testis. The illustrations were drawn by MZ and DX. (b) The scheme for identifying that *F4/80*⁺ cells are critical in TCDT formation. The percentage yield of each population compared to the starting number of live cells derived from testes is indicated. Results are shown as mean ± SD ($n = 5$ for each group). dpp, days post-partum.



TCDTs, the cell suspension were incubated with the Hoechst (final concentration 5 $\mu\text{g/ml}$) and PI (final concentration 2 $\mu\text{g/ml}$) at 37°C for 30 min and were washed with PBS/FBS twice. Samples were all sorted on a BD FACSAria II cell sorter.

Immunohistochemical analysis. The tissues were fixed in 4% paraformaldehyde, frozen in Tissue-Freezing medium, sectioned at a thickness of 10 microns. The sections were stained with primary antibody against MIS, GATA-1, α -SMA, Mvh, CYP17A1 (Cyp17) and c-Kit for one hour at 37°C. After rinsing, sections were incubated for one hour at 37°C with a corresponding secondary antibody. All the antibody information was listed in Table S1. The nuclei were counterstained with Hoechst 33342. The frozen sections from normal testis were used as controls. The experiments were repeated for more than three times. The frozen sections from adult testis were set as positive control and negative control for all antibodies. The experiments were repeated more than three times.

Bisulfite sequencing. The DNA samples extracted from the round sperms and SSCs were enzymatic digested using the restriction enzyme BamHI. The PCR products corresponding to the putative region were amplified from the DNA samples and were cloned into pMD19-T vectors (Takara). The individual clones were sequenced by Invitrogen, Shanghai. Bisulfite primer information is presented in Table S2.

SSC culture and transplantation. For deriving EGFP-SSC lines, the sorted cells were seeded on the mouse embryonic fibroblast (MEF) feeder cells and cultured with the modified SSC medium. The culture medium consisted of StemPro-34 SFM (Invitrogen) supplemented with StemPro supplement (Invitrogen), 25 $\mu\text{g/ml}$ insulin, 100 $\mu\text{g/ml}$ transferrin, 60 μM putrescine, 30 nM sodium selenite, 6 mg/ml D-(+)-glucose, 30 $\mu\text{g/ml}$ pyruvic acid, 1 $\mu\text{l/ml}$ dl-lactic acid (Sigma), 5 mg/ml bovine serum albumin (Sigma), 2 mM L-glutamine, 2-mercaptoethanol (Millipore), minimal essential medium vitamin solution (Invitrogen), non-essential amino acid solution (Millipore), L-glutamine (Millipore), penicillin/streptomycin (Invitrogen), 0.1 mM ascorbic acid, 10 $\mu\text{g/ml}$ d-biotin (Sigma), 20 ng/ml recombinant human epidermal growth factor (Invitrogen), 10 ng/ml human basic fibroblast growth factor (Invitrogen), 10 ng/ml recombinant human glial cell line-derived neurotrophic factor (Invitrogen) and 1% fetal bovine serum (ES cell-qualified, Invitrogen). The cells were maintained at 37°C in an atmosphere of 5% carbon dioxide in air. Culture medium was changed every 2–4 days. All cultured cells were tested to make sure be mycoplasma free. For SSCs transplantation, busulfan (40 mg/kg)-treated 4–6 weeks old F1 male mice were used as the recipient mice. Approximately $2\text{--}3 \times 10^5$ cells were injected with a micropipette (60 μm diameter tips) into the seminiferous tubules of the testes of recipient mice through the efferent duct. The mice were sacrificed 2 months later, and the testes were examined under a fluorescence microscope to detect existence of transplanted SSCs by their EGFP expression.

Intracytoplasmic round spermatid injection (ROSI). Metaphase II-arrested oocytes were collected from superovulated B6D2F1 females (8–10 wks) and cumulus cells were removed using hyaluronidase. Round spermatids and mature sperms were enriched from the TCDTs and reconstituted testes and injected into the oocytes in a droplet of HEPES-CZB medium containing 5 $\mu\text{g/ml}$ cytochalasin B (CB) using a blunt Piezo-driven pipette. The oocytes were then activated by treatment with SrCl₂ for 5–6 hours and maintained in the KSOM medium at 37°C under 5% CO₂ in air. The fertilized oocytes were cultured for 24 h or 3.5 d and two-cell embryos or blastocysts were transferred into the oviducts or uterus of pseudopregnant ICR females, respectively. Live pus retrieved on Day 19.5 were raised by lactating ICR foster mothers.

Quantitative PCR. Total RNA was extracted from the cells using Trizol reagent (Invitrogen). RNA was reverse transcribed using a First Strand cDNA Synthesis kit (TOYOBO, FSK-100). Real-time quantitative PCR reactions were set up in triplicate using SYBR Green Realtime PCR Master Mix (TOYOBO, QPK-212) and run on a Bio-Rad CFX96. All of gene expression levels were normalized to the internal standard gene, *Gapdh*. And results were from three independent experiments. Primer information is provided as Table S2.

Simple sequence length polymorphism (SSLP). The microsatellite markers using in simple sequence length polymorphism (SSLP) were amplified using primers for D1Mit48 and D4Mit15, whose sequences were obtained from the Mouse Genome Informatics website (The Jackson Laboratory, <http://www.informatics.jax.org>). DNA was extracted from cells or tail tips of mice. Thirty-five cycles of PCR amplification were performed and the PCR products were separated on 3% agarose gel before visualization. The experiments were repeated two times.

Immunosuppressing assay. Briefly, the F4/80⁺ cells and F4/80⁻ cells were isolated from the testes or the TCDTs, and seeded into 96-well plates. Non-adherent cells were removed after 24 hrs incubation. For TCDTs, the F4/80⁺ cells were sorted and proliferated in macrophages special medium (MCM) consisting of DMEM/F-12 (Invitrogen), 10% fetal bovine serum (Invitrogen), penicillin/streptomycin and 10 ng/ml M-CSF (Invitrogen) then seeded into 96-well plates. Splenocytes dissected from WT mice were then added in each wells and activated with anti-CD3 and anti-CD28 antibodies for 48 hrs. Activated splenocytes and untreated splenocytes were used as positive and negative controls. Six hours later, each well was pulsed with H₃-thymidine, and proliferation assay were carried out later. The experiments were repeated for three times.

Elisa. To test the concentration of testosterone, we use the mouse testosterone Elisa Kit (Bluegene). The F4/80⁺ and F4/80⁻ cells were cultured in MCM, respectively. 48 h later, the supernatant from F4/80⁺ cells was collected and centrifuged at 1200 rpm for 10 min to remove cells. The resulting supernatant was termed TMCM. The F4/80⁻ cells were then cultured in TMCM. 24 h later, the supernatant was centrifuged at 3000 rpm for 15 minutes to remove debris and used for elisa assay. The experiments were repeated for three times.

Statistic analysis. The weight of TCDTs and the ratios of germ cells in TCDTs were analyzed by unpaired Student's *t* test. All statistical analyses were done by Graphpad primer software 5.0. P value > 0.05 was assumed to be not significant (n.s.). P value < 0.05 was assumed to be statistically significant. “*”: 0.01 < p < 0.05; “**”: 0.001 < p < 0.01; “***”: p < 0.001.

- Lennartsson, J. & Ronnstrand, L. Stem cell factor receptor/c-Kit: from basic science to clinical implications. *Physiol Rev* **92**, 1619–1649 (2012).
- Ronnstrand, L. Signal transduction via the stem cell factor receptor/c-Kit. *Cell Mol Life Sci* **61**, 2535–2548 (2004).
- Orlic, D., Fischer, R., Nishikawa, S., Nienhuis, A. W. & Bodine, D. M. Purification and characterization of heterogeneous pluripotent hematopoietic stem cell populations expressing high levels of c-kit receptor. *Blood* **82**, 762–770 (1993).
- Ogawa, M. *et al.* Expression and function of c-kit in hemopoietic progenitor cells. *J Exp Med* **174**, 63–71 (1991).
- Bearzi, C. *et al.* Human cardiac stem cells. *Proc Nat Acad Sci U S A* **104**, 14068–14073 (2007).
- Tallini, Y. N. *et al.* c-kit expression identifies cardiovascular precursors in the neonatal heart. *Proc Nat Acad Sci U S A* **106**, 1808–1813 (2009).
- Beltrami, A. P. *et al.* Adult cardiac stem cells are multipotent and support myocardial regeneration. *Cell* **114**, 763–776 (2003).
- Kajstura, J. *et al.* Evidence for human lung stem cells. *N Engl Med* **364**, 1795–1806 (2011).
- Offredo, F. S., Steinhilber, M. L., Gannon, J. & Lee, R. T. Bone marrow-derived cell therapy stimulates endogenous cardiomyocyte progenitors and promotes cardiac repair. *Cell stem cell* **8**, 389–398 (2011).
- Mauduit, C., Hamamah, S. & Benahmed, M. Stem cell factor/c-kit system in spermatogenesis. *Hum Reprod Update* **5**, 535–545 (1999).
- Sette, C., Dolci, S., Geremia, R. & Rossi, P. The role of stem cell factor and of alternative c-kit gene products in the establishment, maintenance and function of germ cells. *Int J Dev Biol* **44**, 599–608 (2000).
- Zhang, L. *et al.* c-kit and its related genes in spermatogonial differentiation. *Spermatogenesis* **1**, 186–194 (2011).
- Orr-Urtreger, A. *et al.* Developmental expression of c-kit, a proto-oncogene encoded by the W locus. *Development* **109**, 911–923 (1990).
- Schrans-Stassen, B. H., van de Kant, H. J., de Rooij, D. G. & van Pelt, A. M. Differential expression of c-kit in mouse undifferentiated and differentiating type A spermatogonia. *Endocrinology* **140**, 5894–5900 (1999).
- Yoshinaga, K. *et al.* Role of c-kit in mouse spermatogenesis: identification of spermatogonia as a specific site of c-kit expression and function. *Development* **113**, 689–699 (1991).
- Shinohara, T., Orwig, K. E., Avarbock, M. R. & Brinster, R. L. Spermatogonial stem cell enrichment by multiparameter selection of mouse testis cells. *Proc Nat Acad Sci U S A* **97**, 8346–8351 (2000).
- Kubota, H., Avarbock, M. R. & Brinster, R. L. Spermatogonial stem cells share some, but not all, phenotypic and functional characteristics with other stem cells. *Proc Nat Acad Sci U S A* **100**, 6487–6492 (2003).
- Shinohara, T., Avarbock, M. R. & Brinster, R. L. beta1- and alpha6-integrin are surface markers on mouse spermatogonial stem cells. *Proc Nat Acad Sci U S A* **96**, 5504–5509 (1999).
- Dores, C., Alpaugh, W. & Dobrinski, I. From in vitro culture to in vivo models to study testis development and spermatogenesis. *Cell Tissue Res* **349**, 691–702 (2012).
- Kita, K. *et al.* Production of functional spermatids from mouse germline stem cells in ectopically reconstituted seminiferous tubules. *Biol Reprod* **76**, 211–217 (2007).
- Honaramooz, A., Megee, S. O., Rathi, R. & Dobrinski, I. Building a testis: formation of functional testis tissue after transplantation of isolated porcine (Sus scrofa) testis cells. *Biol Reprod* **76**, 43–47 (2007).
- Arregui, L. *et al.* Xenografting of sheep testis tissue and isolated cells as a model for preservation of genetic material from endangered ungulates. *Reproduction* **136**, 85–93 (2008).
- Bastos, H. *et al.* Flow cytometric characterization of viable meiotic and postmeiotic cells by Hoechst 33342 in mouse spermatogenesis. *Cytometry A* **65**, 40–49 (2005).
- Yang, H. *et al.* Generation of genetically modified mice by oocyte injection of androgenetic haploid embryonic stem cells. *Cell* **149**, 605–617 (2012).
- Oatley, J. M. & Brinster, R. L. The germline stem cell niche unit in mammalian testes. *Physiol Rev* **92**, 577–595 (2012).
- Kanatsu-Shinohara, M., Toyokuni, S. & Shinohara, T. CD9 is a surface marker on mouse and rat male germline stem cells. *Biol Reprod* **70**, 70–75 (2004).
- Hofmann, M. C., Braydich-Stolle, L. & Dym, M. Isolation of male germ-line stem cells; influence of GDNF. *Dev Biol* **279**, 114–124 (2005).



28. Meng, X. *et al.* Regulation of cell fate decision of undifferentiated spermatogonia by GDNF. *Science* **287**, 1489–1493 (2000).
29. Kanatsu-Shinohara, M. *et al.* Long-term proliferation in culture and germline transmission of mouse male germline stem cells. *Biol Reprod* **69**, 612–616 (2003).
30. Gnassi, L. *et al.* Leydig cell loss and spermatogenic arrest in platelet-derived growth factor (PDGF)-A-deficient mice. *J Cell Biol* **149**, 1019–1026 (2000).
31. Barroca, V. *et al.* Mouse differentiating spermatogonia can generate germinal stem cells in vivo. *Nat Cell Biol* **11**, 190–196 (2009).
32. Manova, K., Nocka, K., Besmer, P. & Bachvarova, R. F. Gonadal expression of c-kit encoded at the W locus of the mouse. *Development* **110**, 1057–1069 (1990).
33. Griswold, S. L. & Behringer, R. R. Fetal Leydig cell origin and development. *Sex Dev* **3**, 1–15 (2009).
34. Cohen, P. E., Nishimura, K., Zhu, L. & Pollard, J. W. Macrophages: important accessory cells for reproductive function. *J Leukoc Biol* **66**, 765–772 (1999).
35. Winnall, W. R. & Hedger, M. P. Phenotypic and functional heterogeneity of the testicular macrophage population: a new regulatory model. *J Reprod Immunol* **97**, 147–158 (2013).
36. Hume, D. A., Halpin, D., Charlton, H. & Gordon, S. The mononuclear phagocyte system of the mouse defined by immunohistochemical localization of antigen F4/80: macrophages of endocrine organs. *Proc Natl Acad Sci U S A* **81**, 4174–4177 (1984).
37. Itoh, M., Xie, Q., Miyamoto, K. & Takeuchi, Y. F4/80-positive cells rapidly accumulate around tubuli recti and rete testis between 3 and 4 weeks of age in the mouse: an immunohistochemical study. *Am J Reprod Immunol* **42**, 321–326 (1999).
38. Zhang, X., Goncalves, R. & Mosser, D. M. The isolation and characterization of murine macrophages. *Curr Protoc Immunol* **Chapter 14**, Unit 14 11 (2008).
39. Mosser, D. M. & Edwards, J. P. Exploring the full spectrum of macrophage activation. *Nat Rev Immunol* **8**, 958–969 (2008).
40. Fadok, V. A. *et al.* Macrophages that have ingested apoptotic cells in vitro inhibit proinflammatory cytokine production through autocrine/paracrine mechanisms involving TGF- β , PGE $_2$, and PAF. *J Clin Invest* **101**, 890–898 (1998).
41. DeFalco, T., Takahashi, S. & Capel, B. Two distinct origins for Leydig cell progenitors in the fetal testis. *Dev Biol* **352**, 14–26 (2011).
42. Ren, G. *et al.* Mesenchymal stem cell-mediated immunosuppression occurs via concerted action of chemokines and nitric oxide. *Cell Stem Cell* **2**, 141–150, doi:10.1016/j.stem.2007.11.014 (2008).
43. Hutson, J. C., Garner, C. W. & Doris, P. A. Purification and characterization of a lipophilic factor from testicular macrophages that stimulates testosterone production by Leydig cells. *J Androl* **17**, 502–508 (1996).
44. Hayashi, K., Ohta, H., Kurimoto, K., Aramaki, S. & Saitou, M. Reconstitution of the mouse germ cell specification pathway in culture by pluripotent stem cells. *Cell* **146**, 519–532 (2011).
45. Hayashi, K. *et al.* Offspring from oocytes derived from in vitro primordial germ cell-like cells in mice. *Science* **338**, 971–975 (2012).
46. Rodriguez-Sosa, J. R. & Dobrinski, I. Recent developments in testis tissue xenografting. *Reproduction* **138**, 187–194 (2009).
47. Gassei, K., Schlatt, S. & Ehmcke, J. De novo morphogenesis of seminiferous tubules from dissociated immature rat testicular cells in xenografts. *J Androl* **27**, 611–618 (2006).
48. Hadley, M. A., Byers, S. W., Suarez-Quian, C. A., Kleinman, H. K. & Dym, M. Extracellular matrix regulates Sertoli cell differentiation, testicular cord formation, and germ cell development in vitro. *J Cell Biol* **101**, 1511–1522 (1985).
49. Hedger, M. P. Macrophages and the immune responsiveness of the testis. *J Reprod Immunol* **57**, 19–34 (2002).
50. Bergh, A., Damber, J. E. & van Rooijen, N. Liposome-mediated macrophage depletion: an experimental approach to study the role of testicular macrophages in the rat. *J Endocrinol* **136**, 407–413 (1993).
51. Gaytan, F. *et al.* In vivo manipulation (depletion versus activation) of testicular macrophages: central and local effects. *J Endocrinol* **150**, 57–65 (1996).
52. Cohen, P. E., Chisholm, O., Arceci, R. J., Stanley, E. R. & Pollard, J. W. Absence of colony-stimulating factor-1 in osteopetrotic (csfmop/csfmop) mice results in male fertility defects. *Biol Reprod* **55**, 310–317 (1996).
53. Hutson, J. C. Physiologic interactions between macrophages and Leydig cells. *Exp Biol Med* **231**, 1–7 (2006).

Acknowledgments

This study was supported by the Ministry of Science and Technology of China (2014CB964803), the National Natural Science Foundation of China (31225017 and 91319310), the 'Strategic Priority Research Program' of the Chinese Academy of Sciences (XDA01010403) and the Shanghai Municipal Commission for Science and Technology (12JC1409600 and 13XD1404000).

Author contributions

M.Z.: conception and design, collection and assembly of data, data analysis and interpretation, and manuscript writing; H.Z., C.Z., E.Z., J.X., W.L. and D.X.: collection and/or assembly of data; Y.S., C.W., H.W. and D.L.: data analysis and interpretation; J.L.: conception and design, data analysis and interpretation, manuscript writing, financial and administrative support, and final approval of manuscript.

Additional information

Supplementary information accompanies this paper at <http://www.nature.com/scientificreports>

Competing financial interests: The authors declare no competing financial interests.

How to cite this article: Zhang, M. *et al.* The Roles of Testicular C-kit Positive Cells in De novo Morphogenesis of Testis. *Sci. Rep.* **4**, 5936; DOI:10.1038/srep05936 (2014).



This work is licensed under a Creative Commons Attribution-NonCommercial-NoDerivs 4.0 International License. The images or other third party material in this article are included in the article's Creative Commons license, unless indicated otherwise in the credit line; if the material is not included under the Creative Commons license, users will need to obtain permission from the license holder in order to reproduce the material. To view a copy of this license, visit <http://creativecommons.org/licenses/by-nc-nd/4.0/>